

# Functional waters in intraprotein proton transfer monitored by FTIR difference spectroscopy

Florian Garczarek<sup>1</sup> & Klaus Gerwert<sup>1</sup>

Much progress has been made in our understanding of water molecule reactions on surfaces<sup>1</sup>, proton solvation in gas-phase water clusters<sup>2,3</sup> and proton transfer through liquids<sup>4</sup>. Compared with our advanced understanding of these physico-chemical systems, much less is known about individual water molecules and their cooperative behaviour in heterogeneous proteins during enzymatic reactions. Here we use time-resolved Fourier transform infrared<sup>5</sup> spectroscopy (trFTIR) and *in situ* H<sub>2</sub><sup>18</sup>O/H<sub>2</sub><sup>16</sup>O exchange FTIR to determine how the membrane protein bacteriorhodopsin<sup>6</sup> uses the interplay among strongly hydrogen-bonded water molecules, a water molecule with a dangling hydroxyl group and a protonated water cluster<sup>7</sup> to transfer protons. The precise arrangement of water molecules in the protein matrix results in a controlled Grothuss proton transfer, in contrast to the random proton migration that occurs in liquid water. Our findings support the emerging paradigm that intraprotein water molecules are as essential for biological functions as amino acids.

Ever since Grothuss<sup>8</sup> proposed his famous concept of fast proton transfer along water chains about 200 yr ago, physical chemists have been trying to understand exactly how protons migrate in liquid water. Today, the results from high-performance computer simulations show that the interconversion between an Eigen cation<sup>9</sup> (H<sup>+</sup>·(H<sub>2</sub>O)<sub>4</sub>) and a Zundel cation<sup>10</sup> (H<sup>+</sup>·(H<sub>2</sub>O)<sub>2</sub>) leads to proton migration in water<sup>4</sup>. In the Eigen complex the hydronium core (H<sub>3</sub>O<sup>+</sup>) is bound to three H<sub>2</sub>O molecules ((H<sub>3</sub>O<sup>+</sup>)·(H<sub>2</sub>O)<sub>3</sub>), whereas in the Zundel cation the proton fluctuates between two water molecules (H<sub>2</sub>O···H<sup>+</sup>···OH<sub>2</sub>). In contrast to this random proton migration in liquid water, a more controlled proton transfer is crucial to many enzymatic reactions in proteins. Internal water-filled cavities have been discovered in several high-resolution structural models of membrane proteins but their functional role during proton translocation is not yet clear.

An excellent model system in which to study the role of protein internal water molecules is the well-characterized light-driven proton pump bacteriorhodopsin<sup>6</sup>, a seven  $\alpha$ -helical membrane protein in which the chromophore retinal is bound by a protonated Schiff base. The absorption of light induces an all-*trans* to 13-*cis* isomerization of retinal and leads, after a few picoseconds, to a metastable protein state with an excess enthalpy of about 12 kcal mol<sup>-1</sup> (ref. 11) termed the 'K intermediate' (Fig. 1a). The first proton transfer takes place after ~80  $\mu$ s during the transition from the L to M intermediate. A proton transfers from the protonated Schiff base PSB to its counterion D85 at roughly the same time that a proton is released to the extracellular medium from the proton release group located near E204 and E194 (Fig. 1b). D96, located on the proton uptake side, reprotonates the Schiff base in the M to N transition<sup>12</sup> and is itself reprotonated from the cytoplasmic bulk. The proton release group receives a proton from D85 in the back reaction to the ground state. The net reaction is to pump a proton across the membrane.

Structural models of the bacteriorhodopsin ground state at 1.55 Å resolution have identified several internal fixed water molecules<sup>13</sup>. These models are deduced from X-ray diffraction data from crystallized proteins taken at 100 K and therefore represent only a static assembly. To characterize the dynamics of the water molecules in the protein, we simulated bacteriorhodopsin under physiological conditions, namely, at room temperature, in a lipid bilayer and completely surrounded by external water molecules<sup>14</sup>. Two extensive water densities at the extracellular side of bacteriorhodopsin were identified (Fig. 1c). The protonation state and connecting hydrogen bonds of these water molecules are crucial for the properties of internal water clusters in proteins.

We used *in situ* H<sub>2</sub><sup>16</sup>O/H<sub>2</sub><sup>18</sup>O exchange (Fig. 2a) and time-resolved FTIR difference spectroscopy (Fig. 2b–d) at room temperature to monitor the hydrogen-bonding state and protonation changes of internal water clusters during the bacteriorhodopsin photocycle. Figure 1d shows a typical three-dimensional representation of a time-resolved FTIR difference (relative to the ground state) data set for the bacteriorhodopsin photocycle. In such a difference spectrum, the positive bands originate from the formation of intermediates and the negative bands refer to the ground state. The appearance of the positive carbonyl band at 1,762 cm<sup>-1</sup> indicates transient protonation of D85 in the M intermediate. The much broader, negative, 'continuum absorbance' indicates a protonated water cluster, which deprotonates in the M intermediate<sup>15</sup>. The nature of the proton release group has been debated for many years<sup>15,16</sup>, but has now been shown to be a protonated water cluster that is hydrogen-bonded to six side chains, including R82, E194 and E204 and three backbone groups<sup>7</sup>.

In addition to this lower water cluster at the release site, three water molecules have been found in the vicinity of the Schiff base (Fig. 1c, green). Figure 3a shows how these water molecules, together with each carboxylate oxygen of D85 and D212, might constitute a pentagonal structure<sup>17,18</sup> that is hydrogen-bonded to the proton at the Schiff base. Such a pentagonal arrangement is a typical low-energy conformation in water known as a 'cyclic pentamer'<sup>19</sup>. Although the positions of the oxygen atoms (red spheres) of the water molecules can be determined from X-ray experiments, their orientations remain unknown.

In the conformation proposed in Fig. 3a, the hydroxyl group of water W401 does not participate in hydrogen bonding. Such dangling groups are also observed on aqueous surfaces<sup>1</sup>. The hydroxyl stretch vibration of a dangling group shows a very sharp band at frequencies higher (>3,600 cm<sup>-1</sup>) than observed in liquid water (3,500–3,200 cm<sup>-1</sup>) owing to the missing hydrogen bond. A free hydroxyl stretch vibration exists in the bacteriorhodopsin ground state (see ref. 17 and citations therein) at 3,644 cm<sup>-1</sup> (Fig. 2a). This band shifts from 3,644 to 3,633 cm<sup>-1</sup> during *in situ* H<sub>2</sub><sup>16</sup>O/H<sub>2</sub><sup>18</sup>O exchange measurement at room temperature and

<sup>1</sup>Lehrstuhl für Biophysik, Ruhr-Universität Bochum, D-44780 Bochum, Germany.

therefore clearly belongs to a dangling water group. The water must be located inside the protein and its exact position can be determined with mutants. The  $3,644/3,633\text{ cm}^{-1}$  difference band disappears when an asparagine residue (N) replaces the aspartate at position 85 in the D85N mutant. As this mutant alters the hydrogen bonding of the pentagonal arrangement, the dangling group water must belong to the upper water cluster (Fig 1, green) and is most probably W401 as shown in Fig. 3a. A dangling group in the upper water cluster at room temperature is evidence that the water molecules in this cluster are immobilized even under physiological conditions. This is notable, because it has been proposed by quantum chemical calculations that the presence of W401 at this position is responsible for the ionic state of D85 (ref. 18).

The water arrangement undergoes a considerable change after photoexcitation<sup>20</sup>. The dangling hydroxyl group of W401 disappears in the M intermediate (Fig. 2a, green), probably owing to its higher mobility in M as proposed by molecular dynamic simulations<sup>21</sup>. The former free hydroxyl group becomes hydrogen-bonded and the corresponding hydroxyl stretch shifts to lower wavenumbers between  $3,600$  and  $3,200\text{ cm}^{-1}$ , where the overlap with the large background absorbance of the solvent water makes it impossible to resolve. Notably, a new water dangling group absorbing at  $3,671/3,660\text{ cm}^{-1}$  appears. It represents a water at the cytoplasmic side<sup>17</sup> that is involved in the reprotonation of the Schiff base by intruding water molecules<sup>6,22</sup>.

As compared with free hydroxyl groups, the stretching band of hydrogen-bonded hydroxyl groups shows a pronounced shift to lower wavenumbers (red shift) and a strong broadening. Figure 2b shows the time-resolved FTIR difference spectrum between  $3,050$  and  $1,720\text{ cm}^{-1}$  taken  $100\text{--}200\text{ ns}$  and  $3\text{--}10\text{ }\mu\text{s}$  after laser excitation. It represents the changes in the K and L intermediates, respectively. The

black baseline represents the absorbance changes caused by the actinic laser flash, which thermally heats water in the hydrated protein sample<sup>23</sup>. Relative to this black line, there is an additional broad negative band between  $3,000$  and  $2,400\text{ cm}^{-1}$  in both intermediates. A similar absorbance change is observed in low-temperature spectra of the K intermediate of bacteriorhodopsin and it has been proposed that this band consists predominantly of absorptions of strong hydrogen-bonded waters superposed by the N–H stretch of the strong hydrogen-bonded Schiff base<sup>17,24</sup>.

Mutations of D85 and D212 affect the broad water absorbance band, but mutations of residues hydrogen-bonded to the lower clusters S193A, E194Q and E204Q show no effect (Fig. 2b). Hydrogen bonds involving ions are generally stronger than those between water molecules. Because W402 is hydrogen-bonded to the positively charged Schiff base and to the two negatively charged carboxylates, D85 and D212 (see Fig. 3a), it is the most likely candidate responsible for this broad absorbance. The disappearance of this absorption in K and L shows that the retinal isomerization in the primary light reaction weakens the strong hydrogen bonds and that they are not re-established in the L intermediate. This result, obtained under physiological conditions, contrasts with the low-temperature measurements, which show reduced amplitude in L. The low-temperature results led to a proposal of a hydration switch model<sup>25</sup>, which obviously does not describe the situation at room temperature.

The hydroxyl stretch bands seem to shift to and get lost in the absorbance region of the solvent liquid water between  $3,600$  and  $3,200\text{ cm}^{-1}$ . An approximate relationship between a hydroxyl stretch band shift and bond enthalpies<sup>26</sup> yields  $-\Delta H = 0.31(\Delta\nu)^{1/2}$ , where  $\Delta H$  is in  $\text{kcal mol}^{-1}$  and  $\Delta\nu$  is in  $\text{cm}^{-1}$ . The frequency shift of one hydroxyl group from  $\sim 2,800\text{ cm}^{-1}$  to  $\sim 3,400\text{ cm}^{-1}$ , that is, from a strong to an average hydrogen bond, indicates an enthalpy loss of

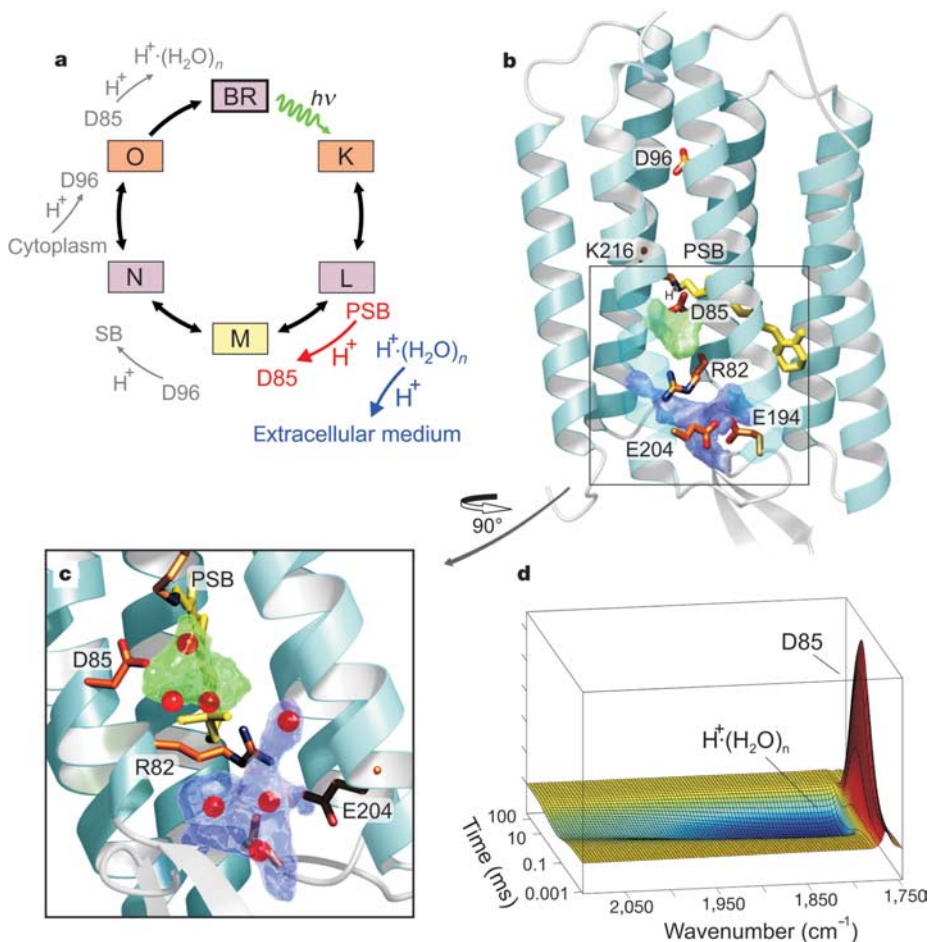


**Figure 1 | Structure and proton transfer steps of bacteriorhodopsin.** **a**, Photocycle scheme showing the main steps in light-driven proton transport. BR, ground state bacteriorhodopsin; PSB, protonated Schiff base. **b**, Structural model of bacteriorhodopsin (PDB code 1C3W; ref. 13) showing its key residues, including the protonated Schiff base by which the chromophore retinal (yellow) is bound to the protein at K216, as well as D85, R82, E194, E204 and D96. The extracellular side shows the space occupied by fluctuating internal water molecules in green (upper water cluster) and blue (lower water cluster)<sup>14</sup>. **c**, Rotation by  $90^\circ$  of the boxed area in **b** to show the position of the water oxygen atoms (red spheres) in the water densities, as determined by X-ray crystallography<sup>13</sup>. The two front helices have been omitted for clarity. **d**, Time-resolved absorbance changes during the photocycle between  $2,100$  and  $1,750\text{ cm}^{-1}$ . At  $1,762\text{ cm}^{-1}$  protonation of D85 (red), and between  $2,100$  and  $1,800\text{ cm}^{-1}$  deprotonation of a water complex (blue), can be followed.

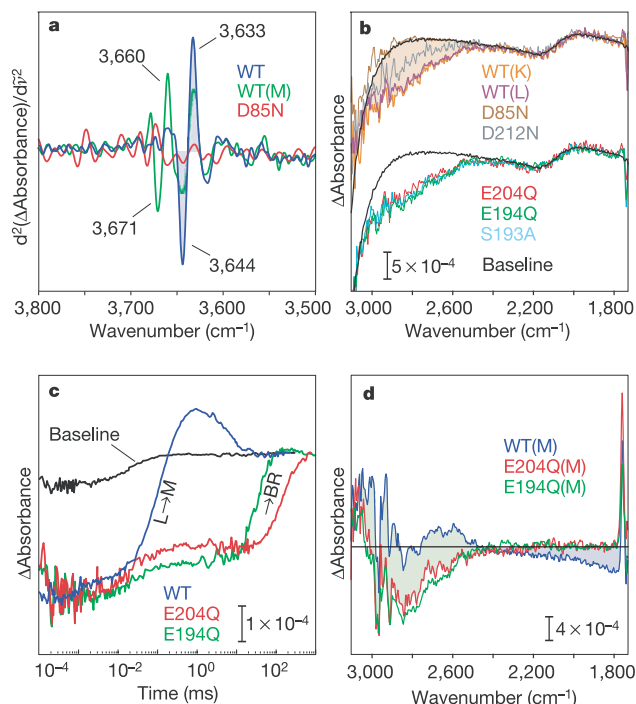


**Figure 2 | FTIR measurements of the internal water molecules of bacteriorhodopsin.** **a**, *In situ*  $\text{H}_2^{16}\text{O}/\text{H}_2^{18}\text{O}$  exchange measurement for wild type (WT) in the ground state (blue), D85N in the ground state (red) and the wild-type M intermediate (intermediate accumulation  $\approx 60\%$ ; green). The vibration of a water dangling hydroxyl group can be identified by its isotopic shift from 3,644 to 3,633  $\text{cm}^{-1}$  in the wild-type ground state. This hydroxyl group is absent in both D85N and the wild-type M intermediate. In the latter, a new difference band appears at 3,671/3,660  $\text{cm}^{-1}$ . **b**, Time-resolved FTIR data in the 3,050–1,720  $\text{cm}^{-1}$  region showing the difference spectra for the K and L intermediates of wild type and for the indicated mutants. The black baseline is not flat owing to the actinic laser flash<sup>23</sup>. The broad negative band (highlighted in red) indicates the breaking of strong hydrogen-bonded water molecules. **c**, Time course of the absorbance changes integrated between 2,900 and 2,600  $\text{cm}^{-1}$  for wild type and two mutants, indicating the breaking ( $\Delta\text{Absorbance} < 0$ ) and merging ( $\Delta\text{Absorbance} \geq 0$ ) of strong hydrogen bonds. BR, ground state bacteriorhodopsin. **d**, As **b**, but for the M intermediate. The absorbance of regenerated strong hydrogen-bonded water is highlighted in green and the continuum absorbance change is highlighted in blue.

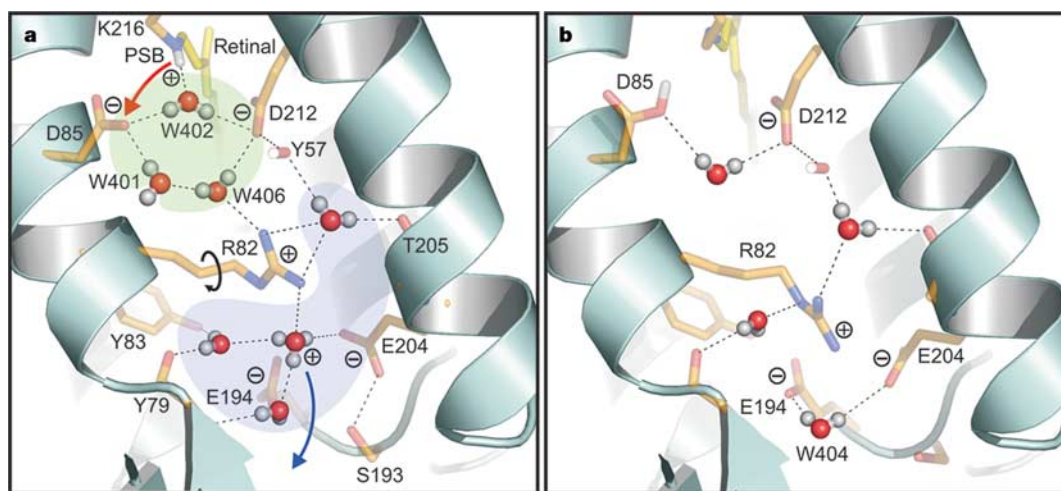


**Figure 3 | Proton transfer via protein internal bound water molecules in the extracellular region of bacteriorhodopsin as derived from the FTIR data.** **a**, Annotation of the area shown in Fig. 1c with water molecules including the hydrogens and catalytic residues (based on PDB 1C3W; ref. 13). Protonation of D85 induces R82 movement. **b**, Structure of the M

about 5.6  $\text{kcal mol}^{-1}$ . Thus, it needs just the weakening of two strong hydrogen bonds to store the K intermediate enthalpy of about 12  $\text{kcal mol}^{-1}$  (ref. 11). The upper water cluster may serve as a temporary energy storage vehicle in the primary photo activation<sup>24</sup>. The enthalpy lost in the primary reaction by the breaking of strong hydrogen bonds could probably be used later during the photocycle for proton transfer.

Figure 2c shows the time dependence of the strong hydrogen-bonded region. The black line again represents the time course of the artificial heat signal. The instantaneous disappearance of the wild-type trace in blue indicates the above-mentioned cleavage of the strong hydrogen bonds in the upper water cluster. Notably, new strong hydrogen bonds form in the L to M transition ( $\sim 80 \mu\text{s}$ ), concomitant with the deprotonation of the water complex at the release site<sup>15</sup>. In E204Q and E194Q mutants of bacteriorhodopsin, by contrast, these strong hydrogen bonds do not form in M, but instead form at the end of the photocycle with a delay in proton release (by a factor of  $\sim 10^3$ ) (refs 6, 16). The strong hydrogen bonds in M might form between W404 and the negatively charged E204 and E194 (Fig. 3b). As expected for such locations, the difference spectra of E204Q and E194Q show deviations as compared with the wild-type protein in the strong hydrogen-bonded region (Fig. 2d, green). The formation of new strong hydrogen bonds among E204, E194 and W404 may provide the enthalpy for release of the proton to the bulk.

The released proton is formally stored in a water cluster (Fig. 3a, blue). Whether the excess proton is stored in a Zundel-like or Eigen-like form remains open. Because the experimentally observed spectra of bacteriorhodopsin agree well with quantum chemical calculations of the spectral dependence of a Zundel cation<sup>27</sup>, but not an Eigen cation, we previously proposed a Zundel-like protonated water complex for bacteriorhodopsin<sup>7</sup>. The calculations give a maximum at  $\sim 2,500 \text{ cm}^{-1}$  for the Eigen cation and at  $\sim 1,800 \text{ cm}^{-1}$  for the Zundel cation, the latter being in agreement with observation. However, mid infrared spectra have now been taken of the protonated water clusters  $\text{H}^+(\text{H}_2\text{O})_n$  with  $2 \leq n \leq 11$  water molecules in the gas phase<sup>3</sup>. Compared with the sharp absorbance bands of the protonated gas-phase water clusters, the bands in bacteriorhodopsin are much broader owing to the coupling with the thermal fluctuating protein environment. The gas-phase measurements show that, in addition to protonated water clusters with  $n = 2$  (Zundel), those with  $n = 3$  and  $n = 5$  also primarily absorb around 1,800  $\text{cm}^{-1}$ , and

intermediate (based on PDB 1C8S; ref. 29). Release of the excess proton is caused by the movement of R82. The strongly hydrogen-bonded water 402, the water molecule with a dangling hydroxyl group (W401) and the protonated water complex are no longer observed in M.

therefore such clusters may also underlie the observed spectral changes in bacteriorhodopsin. The  $n = 3$  cluster forms a hydronium ion ( $\text{H}_3\text{O}^+$ ) that, unlike the classical Eigen cluster, no longer benefits from the symmetrical solvation of three water molecules. An asymmetrically solvated  $\text{H}_3\text{O}^+$  ion is thus as likely as a Zundel cation to be the core of the protonated water cluster of bacteriorhodopsin. At present, we cannot distinguish between these two possibilities or the possibility that the proton fluctuates between both forms at the release site.

Integrating the data from years of experimentation on bacteriorhodopsin<sup>6</sup>, we can propose the following molecular mechanism for proton release. The light induced retinal isomerization breaks the interconnections in the water–aspartate pentamer (Fig. 3a, green), which stores parts of the excitation enthalpy owing to hydrogen-bond cleavage and reduces the pK of the central proton binding site. The latter results in the transfer of a proton from the protonated Schiff Base to D85, which induces a movement of R82 (refs 28, 29, and Fig. 3b). R82 contributes to solvation of the lower protonated water cluster<sup>7,14</sup>. In bacteriorhodopsin, amino acids have the role of the so-called ‘second shell waters’ that solvate protonated waters in liquids. In liquids, the thermal fluctuation-driven release of a water from the second hydration shell, rather than the fast fluctuation of the proton, is rate limiting. With amino acids replacing these waters, the arbitrary release of a second shell water is no longer rate limiting; rather, the protein-controlled R82 movement towards the protonated water cluster determines the proton release owing to electrostatic interactions (Fig. 3b). The pK of the protonated cluster decreases from 9.5 in the ground state to below 5.3 in the M intermediate. The enthalpy for this process might be gained by the formation of new strong hydrogen bonds, probably among W404, E204, E194 and R82 (Fig. 3b).

Similar to the way in which they provide proton transfer in bacteriorhodopsin, single water molecules may transfer protons at the proton uptake side in photosynthetic proteins and also in redox-driven proton pumps such as cytochrome *c* oxidase.

## METHODS

**Mutagenesis and mutant expression.** Purple membrane sheets containing bacteriorhodopsin were isolated and the site-specific mutants were prepared as described<sup>7</sup>.

**Time-resolved measurements.** Time-resolved measurements were made by the step-scan FTIR technique<sup>7</sup>. Purple membranes were suspended (200 µg in 1 M KCl and 100 mM Tris-HCl buffer; pH 7), centrifuged (2 h at 200,000g) and squeezed between two CaF<sub>2</sub> windows. Spectra were taken with a spectral resolution of 4 cm<sup>-1</sup> and a time resolution of 30 ns.

**In situ H<sub>2</sub><sup>16</sup>O/H<sub>2</sub><sup>18</sup>O exchange measurements.** Pure membrane sheets were suspended at a concentration of 5 mg ml<sup>-1</sup> in 0.5 mM KCl and 0.5 mM Tris-HCl buffer (pH 8). Two 10-µl aliquots of this solution were dried on two CaF<sub>2</sub> windows. The experimental procedure was similar to *in situ* H/D exchange measurements<sup>7</sup> except that here isotopically labelled H<sub>2</sub><sup>18</sup>O replaced deuterium dioxide and the measurements were taken at room temperature for the ground state (238 K for the M intermediate). Because of this higher temperature, a larger amount of water vapour was present in the sample. To separate the water vapour bands from the bands of interest, we subtracted a protein-free reference spectrum from the experimental data. To depress the large and broad water absorbance bands of solvent water, the second derivatives of the exchange difference spectra were calculated as described<sup>7</sup> (in brief,  $\frac{d^2}{d\nu^2}\text{H}_2^{16}\text{O}/\text{H}_2^{18}\text{O}$  spectrum).

**Figures.** Figures 1b, c and 3 were prepared with the programs MOLMOL<sup>30</sup>, POV-Ray (<http://www.povray.org>) and PyMOL (<http://www.pymol.org>).

Received 9 August; accepted 8 September 2005.

Published online 9 November 2005.

- Marx, D. Throwing tetrahedral dice. *Science* **303**, 634–636 (2004).
- Zwier, T. S. The structure of protonated water clusters. *Science* **304**, 1119–1120 (2004).
- Headrick, J. M. *et al.* Spectral signatures of hydrated proton vibrations in water clusters. *Science* **308**, 1765–1769 (2005).
- Marx, D., Tuckerman, M. E., Hutter, J. & Parrinello, M. The nature of the hydrated excess proton in water. *Nature* **397**, 601–604 (1999).

- Kötting, C. & Gerwert, K. Proteins in action monitored by time-resolved FTIR spectroscopy. *Chem. Phys. Chem.* **6**, 881–888 (2005).
- Lanyi, J. K. Bacteriorhodopsin. *Annu. Rev. Physiol.* **66**, 665–688 (2004).
- Garczarek, F., Brown, L. S., Lanyi, J. K. & Gerwert, K. Proton binding within a membrane protein by a protonated water cluster. *Proc. Natl Acad. Sci. USA* **102**, 3633–3638 (2005).
- de Grothhuss, C. J. T. Sur la décomposition de l'eau et des corps qu'électrique en dissolution à l'aide de l'électricité galvanique. *Ann. Chim.* **58**, 54–74 (1806).
- Eigen, M. Proton transfer, acid-base catalysis, and enzymatic hydrolysis. Part I: Elementary processes. *Angew. Chem. Int. Edn Engl.* **3**, 1–19 (1964).
- Zundel, G. in *The Hydrogen Bond—Recent Developments in Theory and Experiments* (ed. Sandorfy, C.) 683–766 (Nort-Holland, Amsterdam, 1976).
- Birge, R. R. *et al.* Revised assignment of energy storage in the primary photochemical event in bacteriorhodopsin. *J. Am. Chem. Soc.* **113**, 4327–4328 (1991).
- Gerwert, K., Hess, B., Soppa, J. & Oesterhelt, D. Role of aspartate-96 in proton translocation by bacteriorhodopsin. *Proc. Natl Acad. Sci. USA* **86**, 4943–4947 (1989).
- Luecke, H., Schobert, B., Richter, H. T., Cartailler, J. P. & Lanyi, J. K. Structure of bacteriorhodopsin at 1.55 Å resolution. *J. Mol. Biol.* **291**, 899–911 (1999).
- Kandt, C., Schlitter, J. & Gerwert, K. Dynamics of water molecules in the bacteriorhodopsin trimer in explicit lipid/water environment. *Biophys. J.* **86**, 705–717 (2004).
- Rammelsberg, R., Huhn, G., Lubben, M. & Gerwert, K. Bacteriorhodopsins intramolecular proton-release pathway consists of a hydrogen-bonded network. *Biochemistry* **37**, 5001–5009 (1998).
- Dioumaev, A. K. *et al.* Existence of a proton transfer chain in bacteriorhodopsin: participation of Glu-194 in the release of protons to the extracellular surface. *Biochemistry* **37**, 2496–2506 (1998).
- Shibata, M. & Kandori, H. FTIR studies of internal water molecules in the Schiff base region of bacteriorhodopsin. *Biochemistry* **44**, 7406–7413 (2005).
- Hayashi, S. & Ohmine, I. Proton transfer in bacteriorhodopsin: Structure, excitation, IR spectra, and potential energy surface analyses by an *ab initio* QM/MM method. *J. Phys. Chem. B* **104**, 10678–10691 (2000).
- Liu, K., Brown, M. G., Cruzan, J. D. & Saykally, R. J. Vibration-rotation tunneling spectra of the water pentamer: Structure and dynamics. *Science* **271**, 62–64 (1996).
- Dencher, N. A., Sass, H. J., Buldt, G. Water and bacteriorhodopsin: structure, dynamics, and function. *Biochim. Biophys. Acta* **1460**, 192–203 (2000).
- Grudinin, S., Buldt, G., Gordeliy, V. & Baumgaertner, A. Water molecules and hydrogen-bonded networks in bacteriorhodopsin—molecular dynamics simulations of the ground state and the M intermediate. *Biophys. J.* **88**, 3252–3261 (2005).
- Le Coutre, J., Tittor, J., Oesterhelt, D. & Gerwert, K. Experimental evidence for hydrogen-bonded network proton transfer in bacteriorhodopsin shown by Fourier-transform infrared spectroscopy using azide as catalyst. *Proc. Natl Acad. Sci. USA* **92**, 4962–4966 (1995).
- Garczarek, F., Wang, J., El-Sayed, M. A. & Gerwert, K. The assignment of the different infrared continuum absorbance changes observed in the 3000–1800 cm<sup>-1</sup> region during the bacteriorhodopsin photocycle. *Biophys. J.* **87**, 2676–2682 (2004).
- Hayashi, S., Tajkhorshid, E., Kandori, H. & Schulten, K. Role of hydrogen-bond network in energy storage of bacteriorhodopsin's light-driven proton pump revealed by *ab initio* normal-mode analysis. *J. Am. Chem. Soc.* **126**, 10516–10517 (2004).
- Tanimoto, T., Furutani, Y. & Kandori, H. Structural changes of water in the Schiff base region of bacteriorhodopsin: proposal of a hydration switch models. *Biochemistry* **42**, 2300–2306 (2003).
- Rozenberg, M., Loewenschuss, A. & Marcus, Y. An empirical correlation between stretching vibration redshift and hydrogen bond length. *Phys. Chem. Chem. Phys.* **2**, 2699–2702 (2000).
- Rousseau, R., Kleinschmidt, V., Schmitt, U. W. & Marx, D. Unravelling water network protonation patterns in bacteriorhodopsin by theoretical IR spectroscopy. *Angew. Chem. Int. Edn Engl.* **43**, 4804–4807 (2004).
- Spassov, V. Z., Luecke, H., Gerwert, K. & Bashford, D. pK<sub>a</sub> calculations suggest storage of an excess proton in a hydrogen-bonded water network in bacteriorhodopsin. *J. Mol. Biol.* **312**, 203–219 (2001).
- Luecke, H., Schobert, B., Richter, H. T., Cartailler, J. P. & Lanyi, J. K. Structural changes in bacteriorhodopsin during ion transport at 2 Å resolution. *Science* **286**, 255–260 (1999).
- Koradi, R., Billeter, M. & Wüthrich, K. MOLMOL: a program for display and analysis of macromolecular structures. *J. Mol. Graph.* **14**, 51–55 (1996).

**Acknowledgements** We thank A. Hartz for protein preparation; E. Hofmann and C. Kandt for help with figure preparation; and R. S. Goody and D. Rumschitzki for help with English. This work was funded by the Deutsche Forschungsgemeinschaft.

**Author Information** Reprints and permissions information is available at [npg.nature.com/reprintsandpermissions](http://npg.nature.com/reprintsandpermissions). The authors declare no competing financial interests. Correspondence and requests for materials should be addressed to K.G. ([gerwert@bph.uni-bochum.de](mailto:gerwert@bph.uni-bochum.de)).